Scientia Africana, Vol. 23 (No. 5), December, 2024. Pp 337-348
© Faculty of Science, University of Port Harcourt, Printed in Nigeria *ISSN 1118 – 1931*

SYNTHESIS, CHARACTERISATION, DNA AND ANTIBACTERIAL ACTIVITIES OF CU(I) COMPLEXES OF BIDENTATE QUINOLINYL SCHIFF BASE HAVING TRIPHENYLPHOSPHINE ANCILLARY LIGAND

Odulaja, O.S.[1]*, Adeleke, A.A. [1], Adewuyi, S.[2], Ibilunle, A.A.[1], Sanyaolu, N.O.[1] Yussuf, S.T.[1] and Hashimi, A.M. [1]

- [1] Department of Chemical Sciences, Olabisi Onabanjo University, Ago-Iwoye, P.M.B 2001 Nigeria.
[2] Department of Chemistry, Federal University of Agriculture, Abeokuta, P.M.B 2240, Nigeria.
***Corresponding author E-mail address:** olufemi.odulaja@oouagoiwoye.edu.ng

Received: 20-06-2024
Accepted: 09-01-2025

https://dx.doi.org/10.4314/sa.v23i5.27

Journal Homepage: http://www.scientia-african.uniportjournal.info
Publisher: *Faculty of Science, University of Port Harcourt.*

ABSTRACT

*This work synthesized new biologically active Cu(I) complexes **C1-C3**, obtained from the reaction of Cu(I) nitrate with different bidentate quinolinyl Schiff base ligands (E)-N-(4-bromophenyl)-1-(quinolin-2-yl)methanimine, **L1 ;** (E)-N-(4-chlorophenyl)-1-(quinolin-2-yl)methanimine, **L2** and (E)-1-(quinolin-2-yl)-N-(p-tolyl)methanimine**, L3** with PPh_3 ancillary ligand. The metal complexes with general formula [Cu L(PPh_3)]NO_3, were characterised by UV-Vis, FT-IR, NMR and MS, TGA/DTA and X-ray crystallography. The affinities of complexes to calf thymus-deoxyribuonucleic acid (CT-DNA) were investigated using and UV-Vis spectrometer and in vitro antibacterial activities against Staphylococcus aureus (SA), Escherichia coli (EC), Klebsiella pneumonia (KP) and Pseudomonas aeruginosa (PA) were investigated using agar well diffusion method with ofloxacin as reference. UV-Visible spectra revealed that ligands imino $\pi \rightarrow \pi^*$ transition shifted to longer wavelengths consequent upon coordination to the copper centre. FT-IR result showed bathochromic shift in the imino (C=N) frequencies in the complexes further confirming coordination to the metal centre. The TGA results showed high stability, consistent with the mass spectra of the various m/z of all the complexes and PPh_3 fragments. Novel single crystals obtained in complexes **C2** and **C3** revealed monoclinic crystal systems depicting distorted tetrahedral geometries. Coordination to the metal center was bidentate for all the ligands through the pyridinyl N and imine N in conjunction with triphenylphosphine. In vitro antibacterial studies revealed that all the complexes exhibited stronger antibacterial activity relative to their parent ligands and PPh_3. The study found out that the metal complexes have better DNA binding and antibacterial performances hence could be used as potential chemotherapeutic agents.*

Keywords: Quinoline carboxaldehyde, bidentate, Schiff base, triphenylphosphine, chemotherapeutic.

INTRODUCTION

Combatting infectious and life-threatening diseases remains a challenge due to the preponderance of multidrug resistance and re-emerging infectious diseases (Morse, 2001.). Antimicrobial resistance (AMR) has remained an emerging problem worldwide, posing a global health threat. The once effective antimicrobial drugs against different

microorganisms are no longer effective due to indiscriminate overuse of antimicrobial drugs, inappropriate drug choices, inadequate dosage and poor adherence to treatment instructions (Marston et al., 2016.) Consequently, there is an urgent need to introduce effective antimicrobial agents. The coordination chemistry of copper complexes of Schiff base has been a subject of extensive research over the years (Andruh, 2015.). In spite of reported activity of copper complexes of Schiff bases, the structure and biological activities of these metal complexes of Schiff bases in conjunction with ancillary ligands still has more to be researched into (Ribeiro et al., 2017.). The stabilization of copper(I) by hemilabile ligands such as triphenylphosphines, forms some of the pioneer studies in coordination chemistry (Simkhovich, 2000.). Subsequent work has demonstrated a diversity of structures and stoichiometries (Karp et al., 2020; Shabbir et al., 2016.). The complexation of N'N bidentate Schiff base ligands with triphenylphosphine co-ligand may bring about several structural motifs, hence varied biological activity (Dharmaraj et al., 2001; Viswanathamurthi et al., 2005.). Numerous bidentate Schiff base complexes of copper(I) have been reported, however, the present work focuses on biological activity in the presence of PPh_3 ancillary ligand. Thus, as part of recent investigations of the triphenylphosphine complexes (Griebel et al., 2020.), we report the synthesis of Cu(I) and pyridinyl Schiff base and triphenylphosphine ligand with very high antibacterial activity.

MATERIALS AND METHODS

Synthesis and characterization of ligands L1–L3.

Ligands (E)-N-(4-bromophenyl)-1-(quinolin-2-yl) methanimine, **L1;** (E)-N-(4-chlorophenyl)-1-(quinolin-2-yl)methanimine, **L2** and E)-1-(quinolin-2-yl)-N-(p-tolyl)methanimine**, L3** were synthesized using a modified literature method for related ligands (Sreelatha et al., 2014.).

Synthesis of copper precursor **[Cu(I) $(PPh_3)_2$]**

Bis-(triphenylphosphine) copper(I) nitrate has previously been synthesized, however in this study, a slightly modified procedure was employed (Lobana et al., 1989.) in the *Bis*-(triphenylphosphine) copper(I) nitrate synthesis. Triphenylphosphine (0.524 g, 2 mmol) was added to ethanol in a 250 mL round bottom flask and stirred continuously for 30 minutes at 40 °C until a clear solution was obtained. Copper (I) nitrate (0.13 g, 1 mmol) was added slowly, and the reaction mixture refluxed for 1 h. The round bottom flask and the reaction mixture was transferred and quenched in an ice bath for 25 min and thereafter filtered. A pale blue air–stable crystalline product was formed and allowed to dry overnight.

Synthesis of copper(I) complexes C1-C3

Copper complexes ***C1-C3*** (Scheme 1) were synthesized by addition of methanolic solution of each of **L1 – L3** (1 mmol) to [Cu $(PPh_3)_2]NO_3$ solution (1.0 mmol, ca. 0.65 g) in dichloromethane under constant stirring at 25 °C for 12 h. The precipitates were first isolated from the solution by evaporating the solvents at reduced pressure using a rotary evaporator. The complexes obtained were recrystallized by dissolving the precipitates in dichloromethane. Single crystals suitable for X-ray diffraction analysis were obtained *via* a solvent layering process using diethyl ether onto the dichloromethane solutions of **C1-C3** at room temperature.

X-ray Crystallography

Crystal evaluation and data collection of C1 and C3 were recorded on a Bruker Apex Duo diffractometer equipped with an Oxford Instruments Cryojet operating at 100(2) K and an Incoatec microsource operating at 30 W power. The data were collected with Mo Kα (λ = 0.71073 Å) radiation at a crystal-to-detector distance of 50 mm using omega and phi scans. The structures of 2, 3 and 5 were resolved by the direct method using the SHELXS (Sheldrick, 2015.) program and refined.

Scientia Africana, Vol. 23 (No. 5), December, 2024. Pp 337-348
© Faculty of Science, University of Port Harcourt, Printed in Nigeria *ISSN 1118 – 1931*

ORTEP-3 (Farrugia, 2012.), system software was used to perform the visual crystal structure information. Non hydrogen atoms were first refined isotropically and thereafter by anisotropic refinement with a full-matrix least-squares method based on F^2 using SHELXL (Sheldrick, 2008.). All hydrogen atoms were positioned geometrically, allowed to ride on their parent atoms.

Antimicrobial study

Antibacterial activity studies of complexes **C1-C3** were carried out using the Agar well diffusion method.

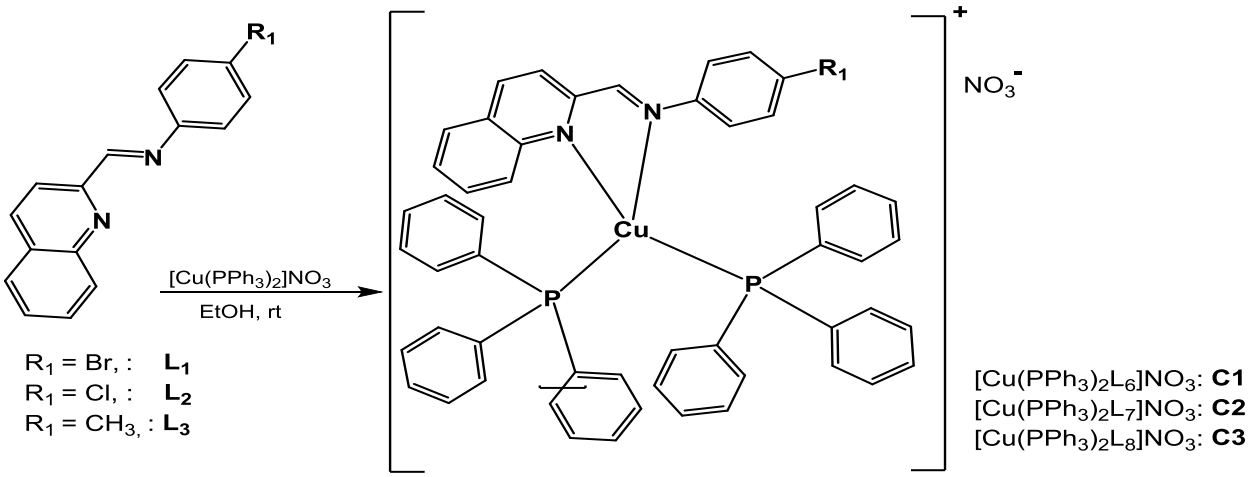

Scheme 1: Synthesis of complexes **C1**–**C3** under constant magnetic stirring in anhydrous ethanol

RESULTS AND DISCUSSION

UV-visible absorption

Electronic absorption spectra recorded in acetonitrile at room temperature in the UV-Vis region of the free ligands **L1**–**L3,** and their corresponding complexes **C1**–**C3** are presented in Figure 1. The absorption spectrum of **L1**, **L2**, and **L3** (Figure 1 a, b and c.) and their respective complexes are similar, showing major absorption band in the UV region between 320–335 nm attributed to intraligand (IL) π–π * transitions. All the complexes bands can be assigned to intra-ligand π–π *, and metal to ligand charge transfer transitions (MLCT) (Dariani et al., 2016.). A significant barthochromic shift in the spectra of **L1**–**L3** complexes was observed, which can be attributed to decrease in energy at the excited states upon coordination to copper(I) (Njogu et al., 2017.) The steric effects of the triphenylphosphine ancillary ligand could have influenced the attenuation observed in the complexes.

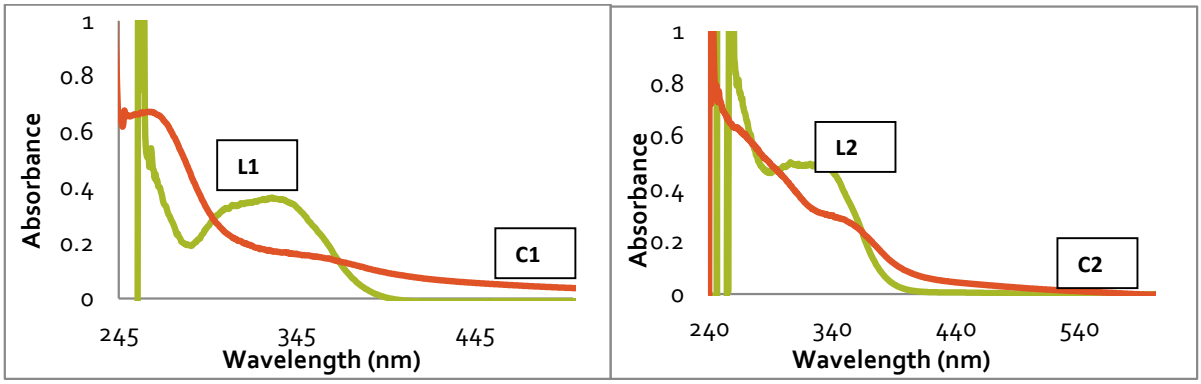

(a) **(b)**

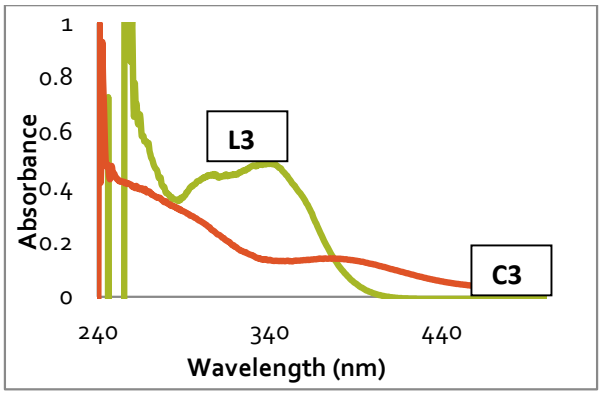

(c)

Figure 1: UV-Vis. spectroscopy of ligand/complex: (a) **L1** /C**1**; (b) **L2**/C**2**; and (c) **L3**/C**3.**

FT-IR Spectroscopy

Coordination of **L1**–**L3** to the Cu(I) centre was confirmed by comparing the FT-IR spectra (Table 1). Frequencies observed between 1621 cm^{-1} associated with the -C=N- bond stretching frequencies shifted to lower frequencies between 1613 cm^{-1} in the spectra of the **L1** and **L2** upon coordination to Cu(I) while in **L3**, the -C=N- band shifted to higher frequencies from 1622 cm^{-1} to 1632 cm^{-1} on coordination to Cu(I). The absorption bands associated with the quinolinyl (C=N) ring in the range 1580–1585 cm^{-1} in the spectra of **L1** and **L2** shifted to the higher frequency on coordination to 1586–1590 cm^{-1}, whereas, in **L3** spectrum, the C=N quinolinyl ring at 1590 cm^{-1} red-shifted to 1584 cm^{-1} on coordination in the spectra of **C3**. Coordination of **L1** – **L3** to Cu(I) can thus be proposed to be bidentate via both N_{imino} and $N_{quinolinyl}$ donor atoms (Abd El-Halim, 2018.). The strong sharp bands observed between 1300 and 1340 cm^{-1} in all the complexes is attributed to the anionic functional group NO_3^-. Moreover, the presence of sharp bands at 1440 – 1460 cm^{-1} in all the complexes is attributable to the presence of PPh_3 (Ramachandran et al., 2012.)

Table 1: Summary of FT-IR Spectra data of imino and quinolinyl functional group of ligands **L1-L3** and their respective Cu(I) complexes **11-13.**

Ligand(Complex)	ν(C=N) cm^{-1}	Δν	ν(qny—N) cm^{-1}	Δν
L1(C**1**)	1621(1613)	08	1584(1589)	05
L2(**C2**)	1621(1614)	07	1583(1587)	04
L3(**C3**)	1622(1632)	10	1590(1584)	06

Table 2: ^{1}H, ^{13}C and ^{31}P NMR chemical shifts in ligands **L1-L3** and complexes **C1-C3**

	^{1}HNMR (**δ** ppm)		^{13}CNMR(**δ** ppm)		^{31}PNMR
Ligand(complex)	Azomethine	Pyridinyl	Azomethine	Pyridinyl	(**δ**ppm)
L1(C1)	8.78(9.26)	8.51(8.87)	160.78(163.33)	156.07(147.39)	0.3939
L2(C2)	8.76(9.26)	8.47(8.85)	162.57(163.53)	155.64(147.59)	0.6215
L3(C3)	8.78(9.25)	8.48(8.85)	160.16(163.70)	159.9(147.10)	0.8613

NMR Spectroscopy

The pattern of coordination is similar in complexes **C1-C3**. The integration values of **L1-L3** revealed that that the complexes adopt a 4-coordinate geometry as observable from the summary of ^{1}H-NMR spectra in Table 2. A significant downfield shift in the imino (HC=N) and alpha protons with respect to the N atom in the quinolinyl ring was observed

Scientia Africana, Vol. 23 (No. 5), December, 2024. Pp 337-348
© Faculty of Science, University of Port Harcourt, Printed in Nigeria *ISSN 1118 – 1931*

compared with their free ligand resonance. In addition, the thirty (30) protons of the two PPh_3 molecules appear as singlet or clusters at δ 7.40-7-00 ppm. The ^{31}P NMR spectra of the complexes suggested that two molecules of triphenylphosphine were coordinated at δ (0.3939-0.8613) ppm. The chemical shift values for the complexes **C1** and **C2** are however less than the value for complex **C3**. The electron-withdrawing substituent in **C1** and **C3** could have influenced this type of observation because electron-withdrawing substituents are known for their ability to reduce electron density around the metal center and thus affects binding interaction between the metal and the donor ligands (Zhu et al., 2018.).

Mass spectroscopy of quinolinyl Cu(I) complexes

The mass spectra of complexes **C1**–**C3** were all obtained in the positive ion mode. Molecular ion peaks m/z = 899 for complex **C1**, attributed to $[CuL1(PPh_3)_2]^+$, complex **C2** base peaks corresponding to $[CuL2(PPh_3)_2]^+$ was observed at m/z 853, while the molecular formula $[CuL3(PPh_3)_2]^+$ corresponded to a prominent molecular ion peak at m/z = 833 for complex **C3**. All spectroscopic studies, along with the elemental analysis, confirmed the formation and purity of the proposed structures in Scheme 1.

X-ray Crystallographic data of Quinolinyl complexes C1 and C3

The crystals of complexes **C1** and **C3** were each grown by layering of diethyl ether unto dichloromethane solution of the complexes. The asymmetric unit of **C1** (Figure 2a,b) has a full molecule of the ligand coordinated to the metal center in a bidentate manner, which consists of one copper (I) center, an ordered ligand, with coordination via the quinoline N atom, the imine N atom in a bidentate manner, one triphenylphosphine P atom and a nitrate anion through O atom to make up a pseudo tetrahedral geometry. Complex **C3** (Figure 3), coordination of the ligand to the metal center was via a N atom of the quinoline moiety, an imine N atom and two triphenylphosphine P atom forming a four-coordinate geometry. Interestingly the nitrate anion is neither coordinated nor observed outside the coordination sphere, the nitrate anion has been dissociated apparently due to the neutral charge of the complex (Table 3). This type of coordination has been observed in related copper(I) complexes (Davis et al., 2015; Obaleye et al., 2021.)

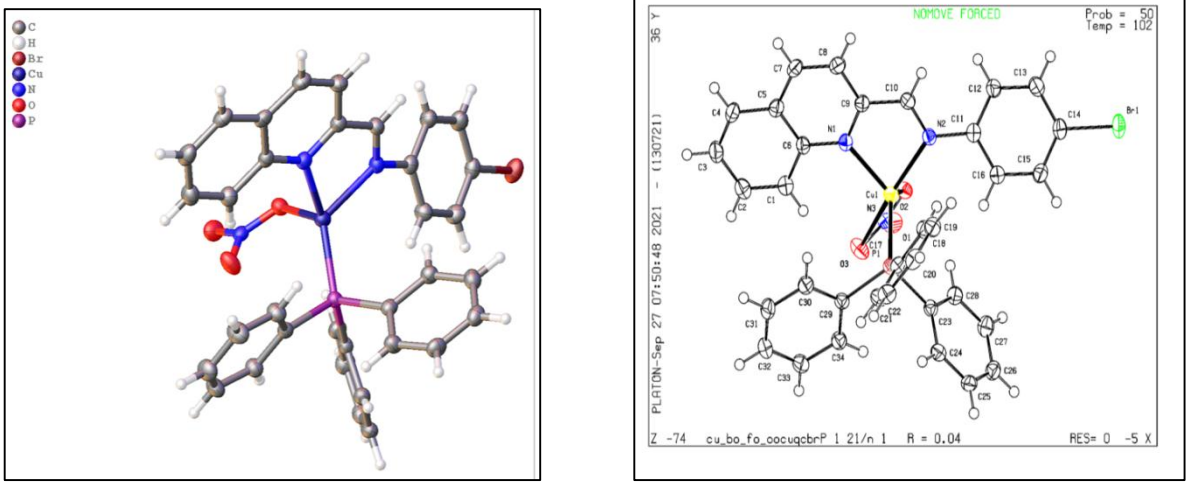

(a) **(b)**

Figure 2: Crystal structure of complex C1 (a) Screen shot (b) Ortep diagram

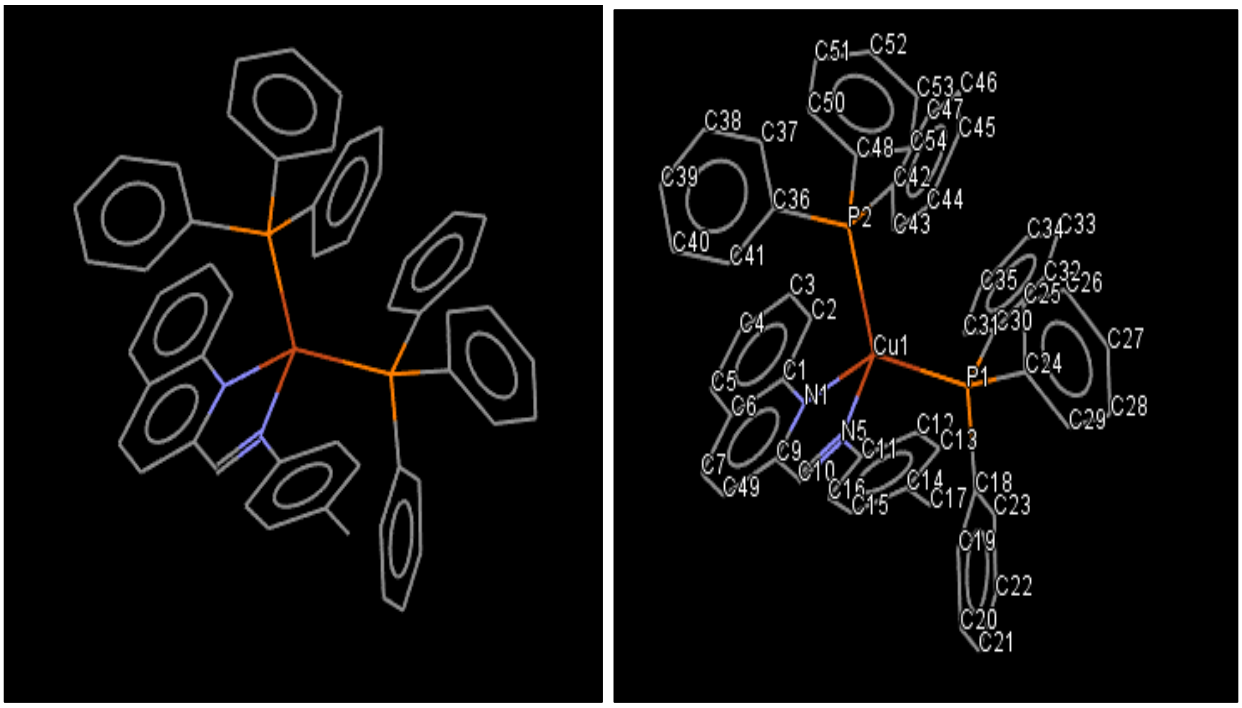

(a) **(b)**

Figure 3: (a) Screenshot and (b) ORTEP diagram of complex **C3**

Table 3: X-ray Crystallographic data of complexes Quinolinyl complexes C1 and C3

	C1	**C3**
Empirical formula	$C_{34}H_{26}BrCuN_3O_3P$	C_{53} H_{43} Cu N_2 P2
Formular weight	699.00	833.38
Temperature:	104 K	103 K
Wavelength	1.54178	1.54178
Crystal system	Monoclinic	Monoclinic
Space group	$P2_{1/n}$	$P\text{-}_1$
a (Å)	8.5763(4)	10.7944(5)
b (Å)	15.8593(7)	12.4884(5))
c (Å)	22.4036(10)	17.7497(7))
α (°)	90	82.304(2)
β (°)	90.386(2)	79.358(2)
ϒ (°)	90	83.709(2)
Volume ($Å^3$)	3047.1(2)	2321.55(17)
Z	4	4
ρ_{calc} g/cm^3	1.524	1.192
μ/mm^{-1}	5.296	5.981
F(000)	1409.81	1416.0
θ range for data collection/°	6.954 to 135.358	7.148 to 135.222
Goodness-of-fit on F^2	1.037	1.040
Crystal size/mm	0.275× 0.178 × 0.15	0.17×0.16 × 0.13
Final R indexes [I>=2σ (I)]	R_1 = 0.0189, wR_2 = 0.0450	R_1=0.0211,wR_2 = 0.0526
Indeex ranges	-14 ≤ h ≤ 15, -17 ≤ k ≤ 17, -22 ≤ l ≤ 25	-15 ≤ h ≤ 15, -16 ≤ k ≤ 16, -21 ≤ l ≤ 22
h,k,lmax	15,17,25	15,16,22

Scientia Africana, Vol. 23 (No. 5), December, 2024. Pp 337-348
© Faculty of Science, University of Port Harcourt, Printed in Nigeria *ISSN 1118 – 1931*

Reflections collected	54701	53132
Independent reflections	7018[R_{int} = 0.0338, R_{sigma} = 0.0181]	5671[R_{int} = 0.0394, R_{sigma} = 0.0209]
Final R indexes [all data]	R_1 = 0.0232, wR_2 = 0.0652	0.0530(5671)
Data/restraints/parameters	2146/0/179	
Largestdiff.peak/hole/e Å^{-3}	0.32/-0.31	0.42/-0.36

DNA binding interactions of Quinolinyl Cu(I) Complexes.

In this study, the extent of interaction of the ligands and the complexes with calf thymus DNA (CT-DNA) was examined by monitoring either the hyperchromic or hypochromic effects observed from the electronic titration. Subsequent additions of DNA to the samples revealed prominent hypochromic shifts with intraligand π–π * bands absorption bands between 249 and 372 nm in the absorption spectra of the ligands and complexes investigated. The hypochromism observed is attributed to significantly strong stacking interaction between the quinolinyl aromatic chromophore and the base pairs of CT-DNA which is as a result of intercalation binding mode of the compounds to CT-DNA. Intercalators are molecules that stack at right angles to the DNA backbone without forming covalent bonds or breaking up the hydrogen bonds between DNA base pairs. The intrinsic binding constant of complexes **C1**–**C2** were evaluated using the Wolfe–Shimer equation (Equation (3)) by determining the ratio of the slope to the intercept from the plot of [DNA]/(εa − εf) versus [DNA]. The binding affinities of the metal salts and free ligands were lower than those of complexes **C1**–**C3**, an indication that the ligands binding affinities were enhanced on complexation to Cu(I). The binding constant obtained ranged between 1.57 × 10^6 and 2.67 × 10^6 M^{-1} for **C1**– **C3.** Complex **C1** had the lowest binding value with a calculated intrinsic binding constant (CIBC) of 1.57 × 10^6 (Figure 4) while complex **C3** has the moderately high binding affinity with a CIBC of 2.27 × 10^6 M^{-1} (Figure 6). The highest binding affinity recorded from complex **C2** (Figure 7) (Kb = of 2.67 × 10^6 M^{-1}). The high binding affinities value obtained for the complexes **C1**–**C3** could be attributed to the interactions of the quinolinyl π-electron with the base pairs of the DNA, and the presence of electron-withdrawing bromine and chlorine sustituents in para-position in ligand **L1** and **L2** (Murugavel et al., 2017.). The influence of triphenylphosphine moiety could also have accounted for the significantly high binding affinities of the complexes. For instance, complex **C1** with least binding affinity has one triphenylphosphine moiety while each of complexes **C2** and **C3** has two (2) triphenylphosphine moieties. High binding affinities have been reported for complexes with electron withdrawing group. This interaction stabilizes the aromatic environment of the CT-DNA base pairs resulting in strong structural perturbations in the DNA molecule resulting in elongation of the distance between the adjacent base pairs (Adeleke et al., 2022.) The order of the DNA binding interaction of the complexes are **C2** > **C3** > **C1**.

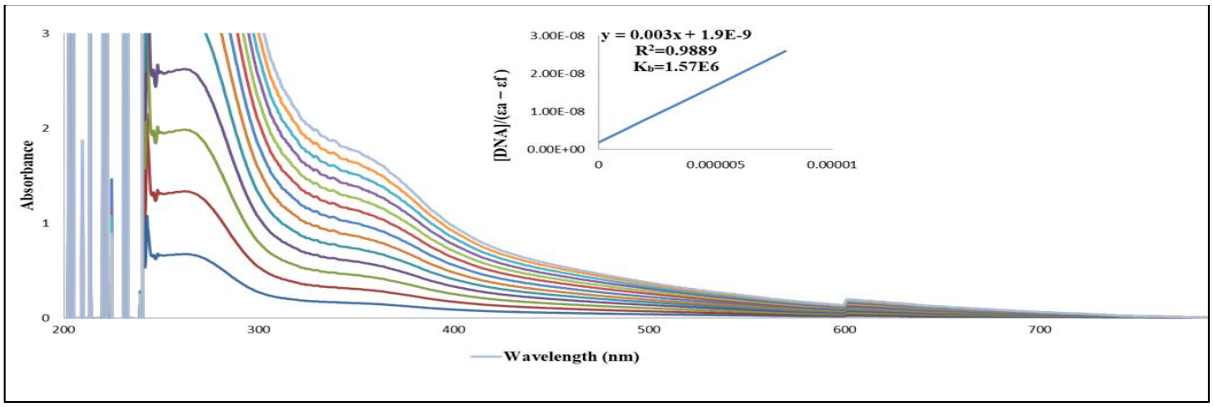

Figure 4: Electronic Absorption Spectra of complex **C1** in the presence of different concentrations of CT-DNA at 350 nm λmax. (insets) A stern-Volmer plot of interactions with CT- DNA. (K_b= 1.57 × 10^6 M^{-1})

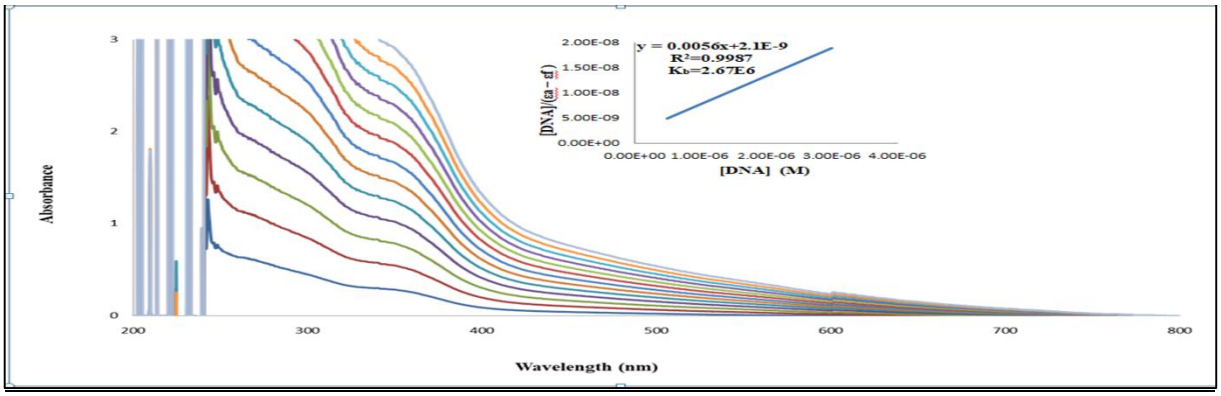

Figure 5: Electronic Absorption Spectra of complex **C2** in the presence of different concentrations of CT-DNA at 350 nm λmax. (insets) A stern-Volmer plot of interactions with CT- DNA. (K_b= 2.67 × 10^6 M^{-1})

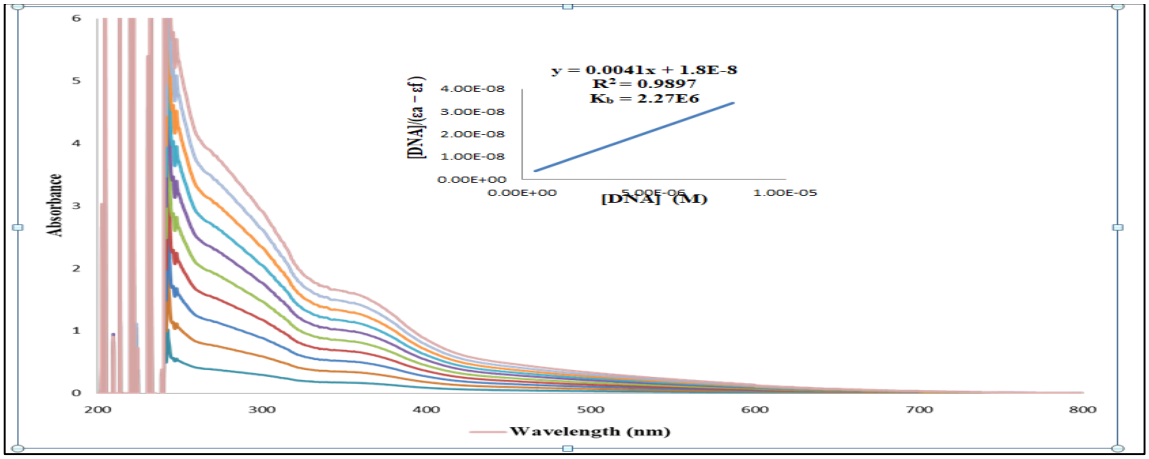

Figure 6**:** Electronic Absorption Spectra of complex **C3** in the presence of different concentrations of CT-DNA at 350 nm λmax. (insets) A stern-Volmer plot of interactions with CT- DNA. (K_b= 2.27 × 10^6 M^{-1})

Scientia Africana, Vol. 23 (No. 5), December, 2024. Pp 337-348

ISSN 1118 – 1931

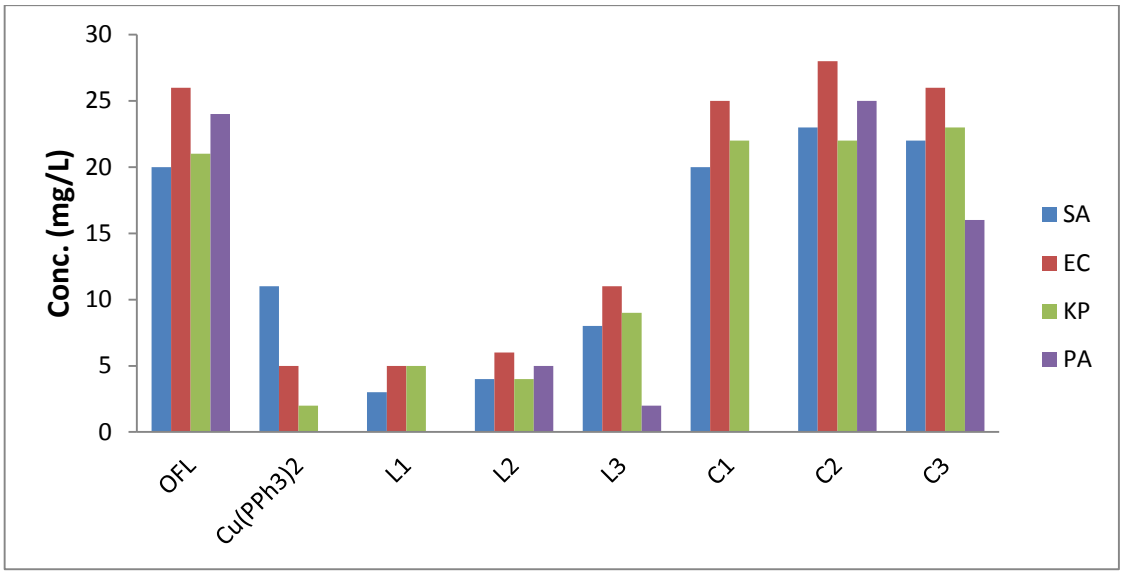

Figure 7: Inhibitory activity of uncomplexed Schiff base ligands L1-L3, ancillary ligand (PPh_3) and respective Cu(I) complexes C1-C3

In-Vitro Antimicrobial Studies

All the ligands, precursor and complexes were tested against one Gram-positive bacteria, Staphylococcus *aureus* (SA), and three Gram-negative bacteria, *Escherichia coli* (EC), *Klebsiella pneumoniae* (KP), and *Pseudomonas aeruginosa* (PA). Ciprofloxacin was used as standard for comparing the minimum inhibitory concentrations activity values. (Figure 7). The sole aim was to investigate the effect of introducing the metal complexes to the bacteria strains. Complexes **C1**–**C3** showed better antibacterial activity compared to **L1–L3** in general, an obvious indication of enhanced activity of the ligands on complexation to $[Cu(PPh_3)_2]$. In addition, copper(I) ion is well known for its bactericidal effects, mechanistically acting by obstruction of bacteria cell functions through direct interaction with the bacteria enzymes, DNA and the negatively charged molecules from the bacterial cell wall. This disrupts cell replication and cell breathing with ultimate result of cell apoptosis through the release of cellular electrolyte into the environment (Adeleke et al., 2021, 2022.). All the ligands showed activity against SA, with highest antibacterial activity exhibited by **L3**. **L1** was active against *EC* and *KP* with an activity value of 5 each, **L2** is active against *EC*, *KP* and *PA* with activity values between 4 and 6, **L3** against *EC, KP* and *PA* with activity values of 11, 9 and 2 respectively. Complexes **C2** and **C3** exhibited the highest antimicrobial activity against all bacteria strains. The ligands of each of **C2** and **C3** consist two molecules of PPh_3, in addition, complex **C2** has a *p*-chloro substituent. Very high antimicrobial activity of compounds containing PPh_3, moiety or the chlorine substituent in the para-position is in agreement with literature report (Desai et al., 2018.) **C1** with only one triphenylphosphine molecule also shows enhanced antimicrobial activity against most of the bacteria strains. All the complexes except **C1** were selectively active against *PA* (compared to other strains) with activity values ranging from 16 to 25, The antibacterial activity of complex **C2** against all the bacterial strains was found to be conspicuously higher than that of the standard *ofloxacin*. Similarly, **C1** and **C3** with an activity value of 20 and 22 signified their better activity than *ofloxacin* against *SA.* This revealed the positive influence of triphenylphosphine on antimicrobial activity.

CONCLUSION

This research work described the synthesis and characterization of copper(I) complexes of three quinolinyl imine. The effect of quinolinyl imine, copper(I) ion, nitrate anion and triphenylphosphine on the interaction of

the compounds were investigated. Molecular structures of all the complexes **C1**, **C2** and **C3** reveal bidentate coordination of the Schiff base to the copper(I) centre, complex **C1** contains in addition to bidentate Schiff base, one PPh_3 molecule and a nitrate (NO_3^-) anion coordinated through O atom to the metal centre, while two molecules of triphenylphosphine were coordinated to the copper(I) centre through P atom in complexes **C2** and **C3** to form a distorted tetrahedral geometry. The nitrate (NO_3^-) remains as counter ion outside the coordination sphere in the case of complexes **C2** and **C3**. CT-DNA binding activities of the free ligands and free metal salts are lower than values obtained for **C1**–**C3**, an indication that the ligands binding affinities were enhanced on complexation to Cu(I). The binding constant obtained in the order **C2** > **C3** > **C1**. Complex **C2** with the highest binding affinity has two PPh_3 moieties while complex **C1** with the least binding affinity has only one triphenylphosphine molecule indicating that triphenylphosphine significantly enhanced the binding affinities of the complexes. This could be attributed to the π-electron interactions of the triphenylphosphine moiety, quinolinyl Schiff base with the base pairs of the DNA, an indication that the compounds bind to CT-DNA via intercalation mode probably due to the assymetric 3-dimensional structure of the complexes. Antimicrobial activity studies reveal that all the ligands exhibited relatively lower activity against the bacterial strains *SA*, *EC* and *KP*. Complexes **C2** and **C3** showed the highest antimicrobial activity against all bacteria strains. Each of the complexes **C2** and **C3** possess two molecules of PPh_3. The antibacterial activity of complexes **C1**, **C2** and **C3** against all the bacterial strains was found to be conspicuously better than that of the standard *ofloxacin*.

Overall, the significant positive influence of triphenylphosphine on antimicrobial activity coupled with the remarkable CT-DNA binding interaction activities recorded for copper(I) quinolinyl Schiff base complexes in conjunction with PPh_3 ancillary ligand unequivocally shows the metal complexes have better DNA binding and antibacterial performances hence could be used as potential anticancer and antibiotic agents.

REFERENCES

Abd El-Halim, H. F., Mohamed, G. G., Anwar, M. N. (2018). Antimicrobial and anticancer activities of Schiff base ligand and its transition metal mixed ligand complexes with heterocyclic base. Applied Organometallic Chemistry, 32(1), e3899.

Adeleke, A. A., Zamisa, S. J., Islam, M. S., Olofinsan, K., Salau, V. F., Mocktar, C., & Omondi, B. (2021). Quinoline functionalized schiff base silver (I) complexes: interactions with biomolecules and in vitro cytotoxicity, antioxidant and antimicrobial activities. Molecules, 26(5), 1205.

Adeleke, A. A., Zamisa, S. J., Islam, M. S., Olofinsan, K., Salau, V. F., Mocktar, C., & Omondi, B. (2022). A study of structure–activity relationship and anion-controlled quinolinyl Ag (I) complexes as antimicrobial and antioxidant agents as well as their interaction with macromolecules. BioMetals, 35(2), 363-394.

Andruh, M. (2015). The exceptionally rich coordination chemistry generated by Schiff-base ligands derived from o-vanillin. Dalton Transactions, 44(38), 16633-16653.

Dariani, R. S., Esmaeili, A., Mortezaali, A., & Dehghanpour, S. (2016). Photocatalytic reaction and degradation of methylene blue on TiO2 nano-sized particles. Optik, 127(18), 7143-7154.

Davis, T. L., Watts, J. L., Brown, K. J., Hewage, J. S., Treleven, A. R., Lindeman, S. V., & Gardinier, J. R. (2015). Structural classification of metal complexes with three-coordinate centres. Dalton Transactions, 44(35), 15408-15412.

Desai, N. C., Vaghani, H. V., Patel, B. Y., & Karkar, T. J. (2018). Synthesis and Antimicrobial Activity of Fluorine

Scientia Africana, Vol. 23 (No. 5), December, 2024. Pp 337-348
© Faculty of Science, University of Port Harcourt, Printed in Nigeria *ISSN 1118 – 1931*

Containing Pyrazole-clubbed Dihydropyrimidinones. Indian Journal of Pharmaceutical Sciences, 80(2), 242-252.

Dharmaraj, N., Viswanathamurthi, P., & Natarajan, K. (2001). Ruthenium (II) complexes containing bidentate Schiff bases and their antifungal activity. Transition metal chemistry, 26(1), 105-109.

Farrugia, L. J. (2012). WinGX and ORTEP for Windows: an update. Journal of applied crystallography, 45(4), 849-854.

Griebel, C., Hodges, D. D., Yager, B. R., Liu, F. L., Zhou, W., Karavage, K. J., Zhu, Y., Norman, S. G., Lan, R., & Day, C. S. (2020). Bisbiphenyl Phosphines: Structure and Synthesis of Gold (I) Alkene π-Complexes with Variable Phosphine Donicity and Enhanced Stability. Organometallics, 39(14), 2665-2671.

Karp, J., Botana, A. S., Norman, M. R., Park, H., Zingl, M., & Millis, A. (2020). Many-body electronic structure of NdNiO 2 and CaCuO 2. Physical Review X, 10(2), 021061.

Lobana, T. S., Bhatia, P. K., & Tiekink, E. R. T. (1989). Synthesis and X-ray crystal structure of chloro [2 (1 H)-pyridinethione-S]-bis (triphenylphosphine) copper (I). Journal of the Chemical Society, Dalton Transactions (4), 749-751.

Marston, H. D., Dixon, D. M., Knisely, J. M., Palmore, T. N., & Fauci, A. S. (2016). Antimicrobial resistance. Jama, 316(11), 1193-1204.

Morse, S. S. (2001). Factors in the emergence of infectious diseases. Plagues and politics, 8-26.

Murugavel, S., Stephen, C. S. J. P., Subashini, R., & AnanthaKrishnan, D. (2017). Synthesis, structural elucidation, antioxidant, CT-DNA binding and molecular docking studies of novel chloroquinoline derivatives: Promising antioxidant and anti-diabetic agents. Journal of Photochemistry and Photobiology B: Biology, 173, 216-230.

Njogu, E. M., Omondi, B., & Nyamori, V. O. (2017). Coordination polymers and discrete complexes of Ag (I)-N-(pyridylmethylene) anilines: Synthesis, crystal structures and photophysical properties. Journal of Coordination Chemistry, 70(16), 2796-2814.

Obaleye, J. A., Lawal, M., Jadeja, R. N., Gupta, V. K., Nnabuike, G. G., Bamigboye, M. O., Roy, H., Yusuff, O. K., & Bhagariya, P. J. I. C. A. (2021). Crystal structure, spectroscopic, DFT calculations and antimicrobial study of the Cu (II) complex bearing second-generation quinolone ofloxacin and 2, 2′-bipyridine. 519, 120264.

Ramachandran, E., Raja, D. S., Bhuvanesh, N. S. P., & Natarajan, K. (2012). Mixed ligand palladium (II) complexes of 6-methoxy-2-oxo-1, 2-dihydroquinoline-3-carbaldehyde 4 N-substituted thiosemicarbazones with triphenylphosphine co-ligand: synthesis, crystal structure and biological properties. Dalton Transactions, 41(43), 13308-13323.

Ribeiro, N., Roy, S., Butenko, N., Cavaco, I., Pinheiro, T., lho, I., Marques, F., Avecilla, F., Pessoa, J. C., & Correia, I. (2017). New Cu (II) complexes with pyrazolyl derived Schiff base ligands: Synthesis and biological evaluation. Journal of Inorganic Biochemistry, 174, 63-75.

Shabbir, M., Akhter, Z., Ahmad, I., Ahmed, S., Shafiq, M., Mirza, B., McKee, V., Munawar, K. S., & Ashraf, A. R. (2016). Schiff base triphenylphosphine palladium (II) complexes: Synthesis, structural elucidation, electrochemical and biological evaluation. Journal of Molecular Structure, 1118, 250-258.

Sheldrick, G. M. (2008). A short history of SHELX. Acta Crystallographica Section A: Foundations of Crystallography, 64(1), 112-122.

Sheldrick, G. M. (2015). Crystal structure refinement with SHELXL. Acta

Crystallographica Section C: Structural Chemistry, 71(1), 3-8.

Simkhovich, L., Galili, N., Saltsman, I., Goldberg, I., Gross, Z.,. (2000). Coordination chemistry of the novel 5, 10, 15-tris (pentafluorophenyl) corrole: Synthesis, spectroscopy, and structural characterization of its cobalt (III), rhodium (III), and iron (IV) complexes. Inorganic Chemistry, 39(13), 2704-2705.

Sreelatha, T., Kandhasamy, S., Dinesh, R., Shruthy, S., Shweta, S., Mukesh, D., Karunagaran, D., Balaji, R., Mathivanan, N., & Perumal, P. T. (2014). Synthesis and SAR study of novel anticancer and antimicrobial naphthoquinone amide derivatives. Bioorganic & medicinal chemistry letters, 24(15), 3647-3651.

Viswanathamurthi, P., Karvembu, R., Tharaneeswaran, V., & Natarajan, K. (2005). Ruthenium (II) complexes containing bidentate Schiff bases and triphenylphosphine or triphenylarsine. Journal of Chemical sciences, 117(3), 235-238.

Zhu, G., Zhang, X., Zhao, M., Wang, L., Jing, C., Wang, P., Wang, X., & Wang, Q. (2018). Influences of fluorine substituents on iminopyridine Fe (II)-and Co (II)-catalyzed isoprene polymerization. Polymers, 10(9), 934.